Axial-Ligand and Metal-Metal Trans Influences in Binuclear Platinum(III) Complexes. Crystal Structures and Spectroscopic Properties of $K_4[Pt_2(P_2O_5H_2)_4(SCN)_2]\cdot 2H_2O$, $K_4[Pt_2(P_2O_5H_2)_4(NO_2)_2]\cdot 2KNO_2\cdot 2H_2O$, and $K_4[Pt_2(P_2O_5H_2)_4(C_3H_3N_2)_2]\cdot 7H_2O$

Chi-Ming Che,*[1a] Wai-Man Lee,[1a] Thomas C. W. Mak,*[1b] and Harry B. Gray[1c]

Contribution from the Department of Chemistry, University of Hong Kong, Hong Kong, Hong Kong, the Department of Chemistry, The Chinese University of Hong Kong, Shatin, New Territories, Hong Kong, and No. 7272 from the Arthur Amos Noyes Laboratory, California Institute of Technology, Pasadena, California 91125. *Received March 8, 1985*

Abstract: The crystal structures of $K_4[Pt_2(pop)_4(SCN)_2]\cdot 2H_2O$ (**1**), $K_4[Pt_2(pop)_4(NO_2)_2]\cdot 2KNO_2\cdot 2H_2O$ (**2**), and $K_4[Pt_2(pop)_4(Im)_2]\cdot 7H_2O$ (**3**) have been determined (pop = diphosphite, $P_2O_5H_2$; ImH = imidazole). Compound **1**: space group $P\bar{1}$, with $a = 9.509$ (7) Å, $b = 9.494$ (5) Å, $c = 9.957$ (5) Å, $\alpha = 117.19$ (4)°, $\beta = 110.88$ (4)°, $\gamma = 94.18$ (4)°, $V = 716.4$ (6) Å^3, and $Z = 1$. Compound **2**: space group $C2/c$, $a = 16.545$ (3) Å, $b = 18.091$ (7) Å, $c = 10.653$ (2) Å, $\beta = 92.80$°, $V = 3185$ (1) Å^3, $Z = 4$. Compound **3**: space group $C2/c$, $a = 19.419$ (8) Å, $b = 10.843$ (4) Å, $c = 16.480$ (8) Å, $\beta = 98.29$ (3)°, $V = 3434$ (2) Å^3, $Z = 4$. The Pt-Pt bond lengths in $[Pt_2(pop)_4(XY)]^{4-}$ complexes vary in the order XY = CH_3I [2.782 (1) Å] > $(SCN)_2$ [2.760 (1) Å] > $(NO_2)_2$ [2.754 (1) Å] > $(Im)_2$ [2.745 (1) Å] > Cl_2 [2.695 (1) Å], a trend that parallels the known trans-influence series for these ligands. The axial platinum-ligand bonds are much longer than normal, revealing that the metal-metal bond also exerts a strong trans influence. With the exception of $[Pt_2(pop)_4(Im)_2]^{4-}$ [$E(\sigma \rightarrow \sigma^*)$, 250 nm], increasing E ($\sigma \rightarrow \sigma^*$) values [345 nm, CH_3I; 282 nm, Cl_2] correlate in a qualitative fashion with decreasing Pt-Pt bond distances.

The electronic structures of $[Pt_2(pop)_4XY]^{4-}$ (pop = $P_2O_5H_2$; XY = Cl_2, Br_2, I_2, CH_3I) complexes all feature Pt-Pt single bonds.[2] Although both the $d\sigma \rightarrow d\sigma^*$ transition energy ($E(\sigma \rightarrow \sigma^*)$, recognizing that both $d\sigma$ and $d\sigma^*$ are mixed with $\sigma(XY)$)[2d] and the ν(Pt-Pt) force constant[3] have been used as indicators of metal-metal bond strength, these indicators are not expected to work very well when the σ orbital is delocalized over the X-Pt-Pt-Y unit.[4] In this paper, with the aid of several crystal structure determinations, we examine the axial bonding interactions and the electronic spectroscopic properties of binuclear platinum(III) complexes.

Experimental Section

Materials. Deionized water was used throughout the experiments. K_2PtCl_4 was purchased from Johnson Matthey and Co., Ltd. All chemicals used were reagent grade. $K_2[Pt_2(SO_4)_4(OH_2)_2]$ was prepared as described in the literature.[5]

$K_4[Pt_2(pop)_4(SCN)_2]\cdot 2H_2O$ (1). This compound was prepared by H_2O_2 oxidation of $K_4[Pt_2(pop)_4]$ in an aqueous solution of KSCN,[2d] and it was recrystallized in hot water.

$K_4[Pt_2(pop)_4(NO_2)_2]\cdot 2KNO_2\cdot 2H_2O$ (2). This complex was prepared by H_2O_2 oxidation of $K_4[Pt_2(pop)_4]$ in an aqueous solution of KNO_2,[2d] followed by recrystallization of the product in hot water. The potassium content in **2** was determined by using a Techtron AA-4 atomic absorption spectrophotometer: found 16.2%, calcd 16.5%.

$K_4[Pt_2(pop)_4(C_3H_3N_2)_2]\cdot 7H_2O$ (3). $[Bu_4N]_4[Pt_2(pop)_4]$ (0.5 g) and excess imidazole (ImH, $C_3H_4N_2$) (1 g) were treated with 30% H_2O_2 (2 mL) in MeOH (20 mL). A yellow crystalline solid gradually deposited upon standing. Dissolution of this species in an aqueous solution of KNO_3 (0.5 g in 20 mL of H_2O) followed by the addition of MeOH yielded **3**, which was recrystallized from H_2O/MeOH (1:1). Anal. Calcd for **3**: N, 4.1; P, 17.9. Found: N, 4.2; P, 18.4. UV-vis: λ_{max}/nm (log ϵ_{max}), 250 (4.52), 270 (4.23), 304 (3.83), 360 (3.5). ^{31}P NMR (in D_2O): δ 26.6 (pseudo t, $^1J_{^{195}Pt-^{31}P} = 2040$ Hz.

$K_4[Pt_2(pop)_4B_2]$ (B = py or nicot; py = pyridine, nicot = nicotinamide). $K_4[Pt_2(pop)_4]$ (0.4 g) and **B** (1 g) in H_2O (15 mL) were treated with excess H_2O_2 (2-3 mL, 15%). After effervescence ceased, the resulting solution was left to stand in air for 15 min. Addition of ethanol to the solution yielded a bright-yellow solid in high yield (>70%). The solid was purified by dissolving it in water, followed by the addition of ethanol or acetone. However, the products were usually contaminated with some monomeric platinum(II) phosphite species, and satisfactory elemental analyses have not been obtained. The ^{31}P NMR spectrum of an aqueous solution of $[Pt_2(pop)_4B_2]^{2-}$ exhibits a pseudotriplet centered at δ 24.0 with $^1J_{^{195}Pt-^{31}P} \sim 2140$ Hz.

Physical Measurements. Electronic absorption spectra were measured at room temperature by using a Beckman Acta CIII spectrophotometer. ^{1}H and ^{31}P NMR spectra were recorded in D_2O on a JEOL FX-90Q FT spectrometer. ^{31}P spectra were referenced to 85% H_3PO_4/D_2O: external standard, H_3PO_4; internal standard, $[Pt_2(pop)_4]^{4-}$.

X-ray Structural Studies. Complexes **1-3** were handled in the same manner. Diffraction measurements were made on a Nicolet R3m four-circle diffractometer (graphite-monochromatized Mo Kα radiation, λ = 0.710 69 Å), and the crystal class, orientation matrix, and accurate unit-cell parameters were determined according to established procedures.[6] The number of hydrated water molecules in each complex was determined from the measured density and later verified in structure refinement.

Intensities were recorded at 22 °C, and data collection and processing parameters are summarized in Table I. Application of absorption corrections was based on a pseudoellipsoidal fit to azimuthal scans of selected strong reflections over a range of 2θ values.[7]

The structures were solved by Patterson and Fourier methods. The binuclear platinum(III) anions in compounds **1-3** all occupy centrosymmetric sites in the crystalline state. The nitrite ions in **2** were found to

(1) (a) University of Hong Kong. (b) The Chinese University of Hong Kong. (c) California Institute of Technology.

(2) (a) Che, C.-M.; Mak, T. C. W.; Gray, H. B. *Inorg. Chem.* **1984**, *23*, 4386-4388. (b) Che, C.-M.; Herbstein, F. H.; Schaefer, W. P.; Marsh, R. E.; Gray, H. B. *J. Am. Chem. Soc.* **1983**, *105*, 4604-4607. (c) Che, C.-M.; Schaefer, W. P.; Gray, H. B.; Dickson, M. K.; Stein, P. B.; Roundhill, D. M. *J. Am. Chem. Soc.* **1982**, *104*, 4253-4255. (d) Che, C.-M.; Butler, L. G.; Grunthaner, P. J.; Gray, H. B. *Inorg. Chem.* **1985**, *24*, 4662-4665. (e) Alexander, K. A.; Bryan, S. A.; Fronczek, F. R.; Fultz, W. C.; Rheingold, A. L.; Roundhill, D. M.; Stein, P.; Watkins, S. F. *Inorg. Chem.* **1985**, *24*, 2803-2808. (f) Clark, R. J. H.; Kurmoo, M.; Dawes, H. M.; Hursthouse, M. B. *Inorg. Chem.* **1986**, *24*, 409-412.

(3) Stein, P.; Dickson, M. K.; Roundhill, D. M. *J. Am. Chem. Soc.* **1983**, *105*, 3489-3493.

(4) (a) Miskowski, V. M.; Schaefer, W. P.; Sadeghi, B.; Santarsiero, B. D.; Gray, H. B. *Inorg. Chem.* **1984**, *23*, 1154-1162. (b) Miskowski, V. M.; Smith, T. P.; Loehr, T. M.; Gray, H. B. *J. Am. Chem. Soc.* **1985**, *107*, 7925-7934.

(5) Orlova, V. S.; Muraveiskaya, G. S.; Evstaf'eva, O. N. *Russ. J. Inorg. Chem.* **1975**, *20*, 753-758.

(6) Sparks, R. A. In *Crystallographic Computing Techniques*, Ahmed, F. R., Ed.; Munksgaard: Copenhagen, **1976**; p 452.

(7) (a) Kopfmann, G.; Huber, R. *Acta Crystallogr., Sect. A* **1968**, *A24*, 348-351. (b) North, A. C. T.; Phillips, D. C.; Mathews, F. S. *Acta Crystallogr., Sect. A* **1968**, *A24*, 351-359.

0002-7863/86/1508-4446$01.50/0

Table I. Dat Collection and Processing Parameters

mol formula	$K_4[Pt_2(P_2O_5H_2)_4(SCN)_2]\cdot 2H_2O$ (**1**)	$K_4[P_2(P_2O_5H_2)_4(NO_2)_2]\cdot 2KNO_2\cdot 2H_2O$ (**2**)	$K_4[Pt_2(P_2O_5H_2)_4(C_3H_3N_2)_2]\cdot 7H_2O$ (**3**)
fw	1274.61	1420.66	1382.66
cell constants			
a, Å	9.509 (7)	16.545 (3)	19.419 (8)
b, Å	9.494 (5)	18.091 (7)	10.843 (4)
c, Å	9.957 (5)	10.653 (2)	16.480 (8)
α, deg	117.19 (4)		
β, deg	110.88 (4)	92.80	98.29 (3)
γ, deg	94.18 (4)		
V, Å^3	716.4 (6)	3185 (1)	3434 (2)
Z	1	4	4
density (flotation in $CCl_4/Br_2CHCHBr_2$), g cm^{-3}	2.96	2.98	2.64
density (calcd)	2.954	2.962	2.674
space group	$P\bar{1}$	$C2/c$	$C2/c$
abs coeff, cm^{-1}	111.07	101.62	91.78
cryst size, mm	0.15 × 0.12 × 0.09	0.36 × 0.28 × 0.24	0.24 × 0.20 × 0.05
mean μr	0.80	1.50	0.40
transmission factors	0.438–0.803	0.023–0.068	0.202–0.481
scan type and speed	ω–2θ; 2.02–14.65	same	same
scan range, deg min^{-1}	1° below $K\alpha_1$ to 1° above $K\alpha_2$	same	same
bkgd	stationary cts for half of the scan time at each end of scan	same	same
collcn range	$h, \pm k, \pm l$; $2\theta_{max} = 54°$	$h,k,\pm l$; $2\theta_{max} = 65°$	$h,k,\pm l$; $2\theta_{max} = 55°$
no. of unique data measd	3012	5012	3278
no. of obsd data with $\|F\| > 3\sigma(\|F\|)$, n	2662	4516	2583
no. of vaiables, p	190	225	231
$F(000)$	597.87	2679.43	2639.42
$R_F = \sum\|\|F_o\| - \|F_c\|\|/\sum\|F_o\|$	0.067	0.035	0.079
weighting scheme	$w = [\sigma^2(\|F_o\|) + 0.0012\|F_o\|^2]^{-1}$	$w = [\sigma^2(\|F_o\|) + 0.0004\|F_o\|^2]^{-1}$	$w = [\sigma^2\|F_o\| + 0.0018\|F_o\|^2]^{-1}$
$R_G = [\sum w(\|F_o\| - \|F_c\|)^2/w\|F_o\|^2]^{1/2}$	0.082	0.041	0.095
$S = [\sum w(\|F_o\| - \|F_c\|)^2/(n-p)]^{1/2}$	1.691	1.362	1.629
residual extrema in final difference map, e Å^{-3}	+6.1 to −3.3	+2.5 to −2.0	+5.2 to −3.0

Table II. Atomic Coordinates (×10^5 for Pt; ×10^4 for Other Atoms) and Equivalent Isotropic Temperature Factors[a] (Å^2 × 10^4 for Pt; Å^2 × 10^3 for Other Atoms) for $K_4[Pt_2(P_2O_5H_2)_4(SCN)_2]\cdot 2H_2O$ (**1**)

atom	x	y	z	U_{eq}
Pt	6973 (6)	10203 (7)	17258 (6)	147 (2)
P(1)	3234 (4)	1242 (5)	1846 (5)	22 (2)
P(2)	1778 (4)	−860 (5)	−1768 (4)	22 (2)
P(3)	832 (4)	−1226 (5)	2136 (5)	21 (2)
P(4)	−641 (4)	−3364 (5)	−1480 (4)	20 (2)
O(1)	3125 (13)	682 (15)	−2 (12)	32 (5)
O(2)	4188 (13)	300 (15)	2467 (13)	30 (5)
O(3)	4261 (13)	3066 (14)	2848 (14)	31 (5)
O(4)	2321 (14)	−2388 (16)	−2123 (15)	34 (6)
O(5)	1895 (14)	−317 (16)	−2991 (14)	33 (6)
O(6)	491 (16)	−2880 (14)	400 (12)	35 (6)
O(7)	−226 (14)	−1586 (14)	2826 (14)	30 (6)
O(8)	2553 (14)	−1069 (15)	3340 (15)	32 (6)
O(9)	−2221 (14)	−4424 (13)	−2015 (13)	29 (5)
O(10)	162 (14)	−4517 (14)	−2534 (13)	30 (5)
K(1)	7109 (5)	2737 (5)	5029 (4)	34 (2)
K(2)	5193 (5)	2595 (5)	−439 (5)	41 (2)
S	1725 (6)	3058 (6)	4754 (5)	38 (2)
C	3420 (24)	2819 (24)	5732 (20)	39 (9)
N	4644 (22)	2759 (26)	6527 (21)	55 (11)
Ow(1)	3003 (17)	4492 (17)	−500 (16)	46 (7)

[a] Calculated as one-third of the trace of the orthogonalized U_{ij} matrix.

Table III. Atomic Coordinates[a] (×10^5 for Pt and P; ×10^4 for Other Atoms) and Temperature Factors[b] (Å^2 × 10^4 for Pt and P; Å^2 × 10^3 for Other Atoms) for $K_4[Pt_2(P_2O_5H_2)_4(NO_2)_2]\cdot 2H_2O$ (**2**)

atom	x	y	z	U_{iso}/U_{eq}
Pt	30535 (1)	20659 (1)	−5830 (2)	171 (1)*
P(1)	20336 (8)	11799 (7)	−10813 (2)	214 (3)*
P(2)	8971 (8)	20724 (8)	1726 (13)	236 (3)*
P(3)	33737 (8)	14112 (8)	13173 (13)	228 (3)*
P(4)	21879 (8)	22887 (8)	25095 (12)	234 (3)*
O(1)	1296 (2)	1275 (2)	−117 (4)	26 (1)*
O(2)	2263 (12)	388 (2)	−963 (4)	30 (1)*
O(3)	1597 (2)	1325 (2)	−2377 (3)	28 (1)*
O(4)	293 (3)	2245 (3)	−904 (4)	34 (1)*
O(5)	402 (3)	1902 (3)	1341 (4)	38 (1)*
O(6)	2610 (2)	1498 (2)	2233 (4)	26 (1)*
O(7)	3512 (3)	600 (2)	1249 (4)	35 (1)*
O(8)	4081 (3)	1773 (3)	2157 (4)	36 (1)*
O(9)	1415 (3)	2082 (3)	3139 (4)	32 (1)*
O(10)	2763 (3)	2680 (3)	3464 (4)	34 (1)*
N(1)	3894 (3)	1374 (3)	−1510 (5)	27 (1)*
O(11)	4559 (3)	1247 (3)	−1017 (5)	43 (2)*
O(12)	3704 (3)	1094 (3)	−2542 (4)	43 (2)*
K(1)	−1036 (1)	3063 (1)	−42 (1)	36 (1)*
K(2)	5000	148 (1)	2500	43 (1)*
K(3)	0	−1092 (1)	2500	57 (1)*
K(4)	2075 (2)	−73 (2)	1447 (2)	112 (1)*
Ow(1)	6220 (3)	449 (3)	618 (5)	47 (2)*
G(1)	1172 (13)	744 (12)	4462 (23)	86 (6)
G(2)	363 (16)	408 (17)	2243 (32)	158 (15)
G(3)	349 (15)	−96 (15)	893 (25)	91 (10)
G(4)	977 (33)	922 (31)	4809 (56)	75 (16)
G(5)	1001 (28)	570 (29)	3461 (52)	97 (21)

[a] Occupancy factors: G(1), 0.82 (8); G(2), 0.54 (3); G(3), 0.39 (2); G(4), 0.28 (8); G(5), 0.24(3). [b] Isotropic temperature, factor exponent: $-8\pi^2U_{iso}\sin^2\theta/\lambda^2$. Asterisk indicates equivalent isotropic temperature factor calculated as one-third of the trace of the orthogonalized U_{ij} matrix.

be badly disordered; they were approximated by fractional oxygen atoms G(1)–G(5) with isotropic temperature factors. The hydrogen atoms of the imidazolyl group in **3** were generated geometrically and included in structure factor calculations with assigned isotropic thermal parameters, but the anionic and water protons in all three Pt(III) compounds were not located.

All computations were performed on a Data General Nova 3/12 minicomputer with the SHELXTL system.[8] Analytic expressions of neutral-atom scattering factors incorporating the real and imaginary components of anomalous dispersion were employed.[9] Blocked-cascade

(8) Sheldrick, G. M. In *Computational Crystallography*; Sayre, D., Ed.; Oxford University: New York, **1982**; p 506.

Table IV. Atomic Coordinates (×10³ for Pt; ×10⁴ for Other Atoms) and Equivalent Isotropic Temperature Factors[a] (Å² × 10⁴ for Pt; Å² × 10³ for Other Atoms) for $K_4[Pt_2(P_2O_5H_2)_4(C_3H_3N_2)_2]\cdot 7H_2O$ (3)

atom	x	y	z	U_{eq}
Pt	29875 (3)	18861 (15)	-3725 (4)	163 (2)
P(1)	2322 (3)	66 (4)	-439 (3)	23 (1)
P(2)	1311 (3)	1328 (4)	367 (4)	25 (2)
P(3)	3554 (3)	1209 (4)	927 (3)	24 (1)
P(4)	2525 (3)	2470 (4)	1685 (3)	23 (1)
O(1)	1807 (6)	116 (9)	248 (8)	20 (4)
O(2)	2719 (7)	-1128 (11)	-259 (11)	34 (5)
O(3)	1777 (8)	-99 (13)	-1239 (10)	44 (5)
O(4)	682 (8)	1256 (12)	-281 (11)	43 (6)
O(5)	1065 (7)	1072 (11)	1190 (11)	38 (5)
O(6)	3035 (8)	1304 (13)	1606 (10)	37 (5)
O(7)	3786 (7)	-126 (13)	1000 (10)	34 (5)
O(8)	4150 (8)	2081 (13)	1297 (10)	44 (6)
O(9)	2945 (9)	3457 (13)	2220 (10)	42 (5)
O(10)	1977 (8)	1947 (13)	2206 (8)	33 (5)
N(1)	3758 (9)	953 (14)	-943 (11)	31 (6)
C(1)	4448 (10)	983 (15)	-715 (15)	30 (6)
N(2)	4747 (8)	224 (14)	-1191 (12)	32 (6)
C(2)	4251 (12)	-340 (19)	-1714 (15)	42 (8)
C(3)	3643 (9)	54 (15)	-1586 (12)	21 (5)
K(1)	388 (3)	917 (4)	3918 (4)	46 (2)
K(2)	2270 (5)	3064 (5)	3758 (4)	77 (3)
Ow(1)	711 (14)	2804 (22)	2916 (17)	95 (11)
Ow(2)	875 (8)	2760 (12)	5010 (11)	42 (6)
Ow(3)	973 (11)	1504 (15)	6576 (13)	64 (7)
Ow(4)	0	-570 (25)	2500	75 (12)

[a] Calculated as one-third of the trace of the orthogonalized U_{ij} matrix.

least-squares refinement[10] converged to the R indices and other parameters listed in Table I.

The final atomic coordinates for compounds 1–3 are given in Tables II–IV, respectively. Selected bond distances and bond angles for complexes 1–3 are compared in Table V. Imidazolyl H coordinates, anisotropic temperature factors, and structure factor tables are available as supplementary material.

Results and Discussion

$[Pt_2(pop)_4B_2]^{n-}$ (B = py, nicot, n = 2; Im, n = 4). In general, diplatinum(III, III) complexes are obtained from oxidative addition reactions of the corresponding diplatinum(II, II) species.[2] Previous experiments have shown that H_2O_2 oxidation of $[Pt_2(pop)_4]^{4-}$ in the presence of nucleophiles produces binuclear platinum(III) complexes in high yield.[2d] A similar procedure has been employed here except that, in the case of complex 3, methanol was used instead of water to prevent hydrolysis of $[Pt_2(pop)_4]^{4-}$.

The $[Pt_2(pop)_4B_2]^{n-}$ species have been characterized by ^{31}P NMR spectra. In all cases, the observed chemical shifts ($\delta \sim 27$–29) and $^1J_{^{195}Pt-^{31}P}$ values (2040–2200 Hz) are typical of platinum(III) diphosphites,[2d] and they closely resemble those of N-bonded $[Pt_2(pop)_4(NO_2)_2]^{4-}$. The intense features in the UV–vis absorption spectra of $[Pt_2(pop)_4(py)_2]^{2-}$, $[Pt_2(pop)_4(nicot)_2]^{2-}$, and $[Pt_2(pop)_4(Im)_2]^{4-}$ are analogous to the strong $\sigma \rightarrow \sigma^*$ absorption at 245 nm in the spectrum[2d] of $[Pt_2(pop)_4(OH_2)_2]^{2-}$. Accordingly, the 250-nm band of $[Pt_2(pop)_4(Im)_2]^{4-}$ is assigned to $\sigma \rightarrow \sigma^*$. Because the N-donor lone pair of Im^- is relatively low energy,[11] LMCT mixing in the $\sigma \rightarrow \sigma^*$ transition of $[Pt_2(pop)_4(Im)_2]^{4-}$ is not expected to be very important. The 270- and 304-nm bands in the $[Pt_2(pop)_4(Im)_2]^{4-}$ spectrum may be due to $\pi(Im) \rightarrow \sigma^*$ transitions; the intraligand $\pi \rightarrow \pi^*$ transition of imidazole has been reported at ~220 nm.[11]

Structures of Complexes 1–3. The centrosymmetric binuclear platinum(III) anions in complexes 1–3 are illustrated in Figures 1–3, respectively. A uniform scheme of atom labeling in the diphosphite ligands has been used, such that O(n) and O(n + 1) denote a pair of terminal oxygen atoms that form shorter and longer bonds, respectively, with their parent phosphorus atom. Each binuclear complex consists of two face-to-face square-planar PtP_4 units linked by four bridging diphosphite groups, with two axial ligands trans to the Pt–Pt bond. As in the case of $[Pt_2(pop)_4Cl_2]^{4-}$[2b] and $[Pt_2(pop)_4CH_3I]^{4-}$,[2a] the PtP_4 unit is essentially square planar (Pt–Pt–P angles in the range 90–92°) with the metal atom slightly displaced toward the other Pt′ atom. As expected, the Pt–Pt distances in complexes 1–3 (2.760 (1), 2.754 (1), and 2.745 (2) Å, respectively) are shorter than those in the unoxidized $[Pt_2(pop)_4]^{4-}$ anion (2.925 (1) Å)[12] and the partially oxidized linear chain $\{[Pt_2(pop)_4Br]^{4-}\}_n$ (2.793 (1) Å),[2b] in accord with σ^*-electron

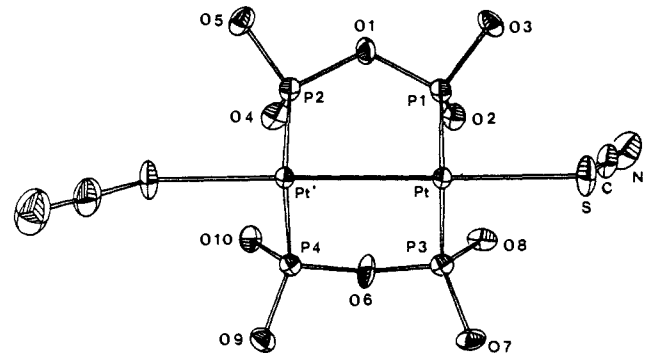

Figure 1. Structure of the centrosymmetric $[Pt_2(P_2O_5H_2)_4(SCN)_2]^{4-}$ anion in 1. For clarity, only two bridging diphosphite ligands are illustrated. The primed atoms are generated from the unprimed ones by the symmetry transformation ($-x$, $-y$, $-z$).

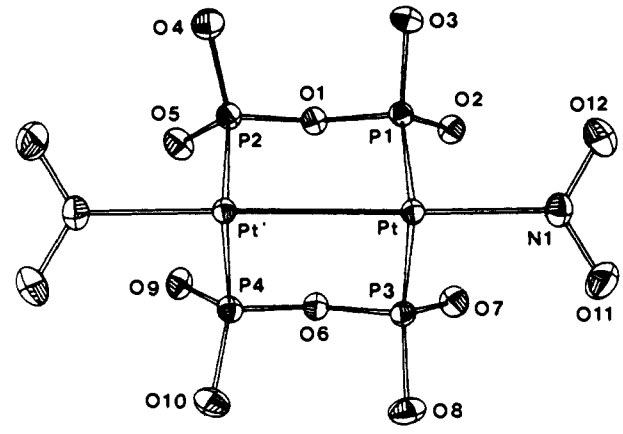

Figure 2. Structure of the centrosymmetric $[Pt_2(P_2O_5H_2)_4(NO_2)_2]^{4-}$ anion in 2. For clarity, two bridging diphosphite ligands have been omitted. The primed atoms are generated from the unprimed ones by the symmetry transformation ($^1/_2 - x$, $^1/_2 - y$, $-z$).

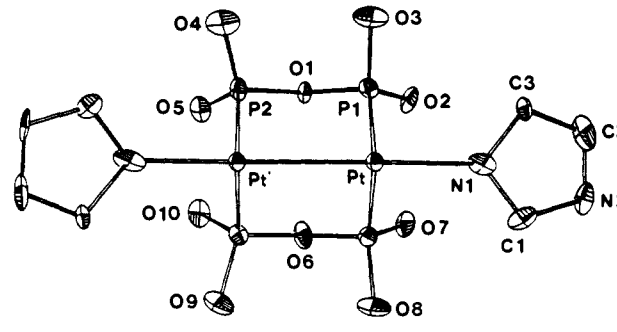

Figure 3. Structure of the centrosymmetric $[Pt_2(P_2O_5H_2)_4(C_3H_3N_2)_2]^{4-}$ anion in 3. For clarity, two bridging diphosphite ligands have been omitted. The primed atoms are generated from the unprimed ones by the symmetry transformation ($^1/_2 - x$, $^1/_2 - y$, $-z$).

(9) *International Tables for X-Ray Crystallography*; Kynoch: Birmingham, England, **1973**; Vol. IV, pp 99, 149.
(10) Schilling, J. W. In *Crystallographic Computing*; Ahmed, F. R., Ed.; Munksgaard: Copenhagen, **1970**; p 201.
(11) Bernarducci, E.; Schwindinger, W. F.; Hughey, J. L., IV; Krogh-Jespersen, K.; Schugar, H. J. *J. Am. Chem. Soc.* **1981**, *103*, 1686–1691.
(12) Filomena Dos Remedios Pintos, M. A.; Sadler, P. J.; Neidle, S.; Sanderson, M. R.; Subbiah, A.; Kuroda, R. *J. Chem. Soc., Chem. Commun.* **1980**, 13–15.

Table V

(a) Common $Pt_2(P_2O_5H_2)_4$ Moiety

	$K_4[P_2(P_2O_5H_2)_4(SCN)_2]\cdot 2H_2O$ (1)	$K_4[Pt_2(P_2O_5H_2)_4(NO_2)]\cdot 2KMO_2\cdot 2H_2O$ (2)	$K_4[Pt_2(P_2O_5H_2)_4(C_6H_3H_2)_2]\cdot 7H_2O$ (3)
Pt–Pt	2.760 (1)	2.754 (1)	2.745 (1)
Pt–P(1)	2.361 (5)	2.369 (2)	2.352 (5)
Pt–P(2)	2.364 (5)	2.358 (2)	2.366 (5)
Pt–P(3)	2.352 (5)	2.383 (2)	2.377 (5)
Pt–P(4)	2.350 (5)	2.378 (2)	2.353 (5)
P(1)–O(1)	1.63 (1)	1.642 (4)	1.62 (2)
P(1)–O(2)	1.49 (1)	1.485 (4)	1.51 (1)
P(1)–O(3)	1.56 (1)	1.548 (4)	1.66 (1)
P(2)–O(1)	1.63 (1)	1.622 (4)	1.51 (2)
P(2)–O(4)	1.51(2)	1.516 (5)	1.53 (2)
P(2)–O(5)	1.56 (2)	1.554 (5)	1.61 (2)
P(3)–O(6)	1.62 (1)	1.642 (4)	1.52 (1)
P(3)–O(7)	1.50 (2)	1.488 (5)	1.55 (2)
P(3)–O(8)	1.59 (1)	1.580 (5)	1.62 (2)
P(4)–O(6)	1.61 (1)	1.625 (4)	1.54 (2)
P(4)–O(9)	1.51 (1)	1.519 (5)	1.57 (2)
P(4)–O(10)	1.59 (1)	1.532 (4)	
			91.0 (1)
P(1)–Pt–Pt	91.8 (1)	90.3 (1)	90.4 (1)
P(3)–Pt–Pt	92.4 (1)	91.5 (1)	92.0 (1)
P(2)–Pt–Pt	91.2 (1)	92.2 (1)	92.3 (1)
P(4)–Pt–Pt	90.8 (1)	91.3 (1)	122.6 (8)
P(1)–O(1)–P(2)	125 (1)	122.3 (5)	123.7 (10)
P(3)–O(6)–P(4)	128 (1)	122.8 (5)	109.3 (4)
Pt–P(1)–O(1)	109.9 (5)	109.4 (2)	107.8 (5)
Pt–P(2)–O(1)	110.6 (5)	108.7 (2)	110.6 (6)
Pt–P(3)–O(6)	110.0 (6)	108.2 (2)	109.8 (6)
Pt–P(4)–O(6)	111.6 (5)	109.4 (2)	116.6 (5)
Pt–P(1)–O(2)	117.6 (6)	117.2 (3)	115.6 (6)
Pt–P(1)–O(3)	112.9 (5)	112.4 (3)	117.0 (6)
Pt–P(2)–O(4)	115.9 (6)	117.1 (3)	113.5 (5)
Pt–P(2)O(5)	112.7 (5)	113.3 (3)	117.4 (6)
Pt–P(3)–O(7)	116.5 (6)	118.5 (3)	112.9 (6)
Pt–P(3)–O(8)	113.3 (6)	113.8 (3)	
Pt–P(4)–O(9)	115.1 (6)	113.1 (3)	116.0 (6)
Pt–P(4)–O(10)	111.3 (6)	114.8 (3)	112.4 (5)

(b) Ligand Geometry and Metal–Ligand Bonding

$K_4[Pt_2(P_2O_5H_2)_4(SCN)_2]\cdot 2H_2O$ (1)		$K_4[Pt_2(P_2O_5H_2)_4(NO_2)]\cdot 2KNO_2\cdot 2H_2O$ (2)		$K_4[Pt_2(P_2O_5H_2)_4(C_3H_3N_2)_2]\cdot 7H_2O$ (3)	
Pt–S = 2.466 (4)	Pt–Pt–S = 172.8 (1)	Pt–N(1) = 2.147 (6)	Pt–Pt–N(1) = 178.7 (2)	Pt–N(1) = 2.13 (2)	N(2)–C(2)–C_3) = 109 (2)
S–C = 1.65 (2)	P(1)–Pt–S = 92.6 (2)	N(1)–O(11) = 1.219 (8)	P(1)–Pt–N(1) = 88.5 (2)	N(1)–C(1) = 1.34 (3)	C(2)–C(3)–N(1) = 107 (2)
C–W = 1.17 (3)	P(3)–Pt–S = 93.3 (2)	N(1)–O(12) = 1.237 (9)	P(3)–Pt–N(1) = 88.8 (2)	C(1)–N(2) = 1.33 (3)	Pt–M(1)–C(1) = 127 (1)
S–C–N = 175 (2)	P(2)–Pt–S = 84.5 (2)	O(11)–N(1)–O(12) = 119.3 (7)	P(2)–Pt–N(1) = 89.0 (2)	N(2)–C(2) = 1.34 (3)	Pt–M(1)–C(3) = 127 (1)
Pt–S–C = 107.7 (7)	P(4)–Pt–S = 83.5 (2)	Pt–N(1)–O(11) = 120.3 (6)	P(4)–Pt–N(1) = 88.5 (2)	C(2)–C(3) = 1.30 (3)	Pt–Pt–N(1) = 179.1 (4)
		Pt–N(1)–O(12) = 120.4 (6)		C(3)–N(1) = 1.43 (2)	P(1)–Pt–N(1) = 89.8 (4)
				C(3)–N(1)–C(1) = 106 (2)	P(3)–Pt–N(1) = 89.3 (5)
				N(1)–C(1)–N(2) = 109 (2)	P(2)–Pt–N(1) = 87.2 (4)
				C(1)–N(2)–C(2) = 109 (2)	P(4)–Pt–N(1) = 88.0 (5)

(c) Coordination of K^+ Ions

$K_4[Pt_2(P_2O_5H_2)_4(SCN)_2]\cdot 2H_2O$ (1)	$K_4[Pt_2(P_iO_5H_2)_4(NO_2)]\cdot 2KNO_2\cdot 2H_2O$ (2)	$K_4[Pt_2(P_2O_5H_2)_4(C_3H_3N_2)_2]\cdot 7H_2O$ (3)
K(1) surrounded by N at 3.19 Å and by O at 2.70, 2.74, 2.77, 2.86, 2.95, 3.01, and 3.03 Å [or 0.02 Å] K (2) surrounded by N at 2.96 Å, by O at 2.83, 2.86, and 2.89 Å, and by Ow at 2.70 and 2.85 Å [or 0.02 Å]	K(1) surrounded by O at 2.79, 2.83, 2.84, 2.92, 3.01, and 3.12 Å and by Ow at 2.78 Å [$\sigma \sim$ 0.01 Å] K(2) surrounded by O at 2.86 × 2), 3.08 (×2), and 3.10 (×2) Å and by Ow at 2.96 (×2) Å [σ 0.001 Å] K(3) surrounded by O at 2.67 (×2) and 2.72 (×2) Å [σ 0.01 Å] and by G at 2.57 (×2) and 2.80 (×2) Å [σ 0.03 Å], K(4) surrounded by O at 2.69, 2.72, 2.73, 2.82, and 3.08 Å[σ 0.01 Å] and by G at 2.81, 2.89, 2.90, 3.08, and 3.12 Å σ 0.03 Å]	K(1) surrounded by O at 2.72, 2.81, and 2.89 Å, and by Ow at 2.76, 2.76, and 2.85 Å [σ 0.02 Å] K(2) surrounded by O at 2.62, 2.72, 2.81, 2.91, 3.05, and 3.16 Å and by Ow at 3.16 Å σ 0.02 Å]

depopulation from Pt(II) to Pt(III): $[Pt_2(pop)_4]^{4-}$, $(\sigma)^2(\sigma^*)^2$; $[Pt_2(pop)_4Br]^{4-}$, $(\sigma)^2(\sigma^*)^1$; $[Pt_2(pop)_4X_2]^{4-}$, $(\sigma)^2$. The Pt–Pt bond length in the $[Pt_2(pop)_4XY]_{4-}$ species decreases in the order XY = CH_3I > $(SCN)_2$ > $(NO_2)_2$ > $(Im)_2$ > Cl_2 (Table VI), which parallels the corresponding decrease in axial-ligand donor strength in a fashion similar to the established structural trans-influence

Table VI. Geometric Properties of the X-Pt-Pt-X System in Binuclear Platinum(III) Complexes

complex	Pt-Pt, Å	Pt-X (axial), Å	ref
$K_4[Pt_2(P_2O_5H_2)_4Cl_2]\cdot 2H_2O$	2.695 (1)	2.407 (2) (Cl^-)[a]	2b
$K_4[Pt_2(P_2O_5H_2)_4(Im)_2]\cdot 7H_2O$	2.745 (1)	2.13 (2) (Im^-)[a]	b
$K_4[Pt_2(P_2O_5H_2)_4(NO_2)_2]\cdot 2KNO_2\cdot 2H_2O$	2.754 (1)	2.147 (6) (NO_2^-)[a]	b
$K_4[Pt_2(P_2O_5H_2)_4(SCN)_2]\cdot 2H_2O$	2.760 (1)	2.466 (4) (SCN^-)[a]	b
$K_4[Pt_2(P_2O_5H_2)_4CH_3I]\cdot 2H_2O$	2.782 (1)	2.18 (3) (CH_3^-), 2.816 (3) (I^-)	2a
$[Pt_2(NH_3)_4(C_5H_4NO)_2Cl_2](NO_3)_2$	2.568 (1)	2.44 (2) (Cl^-), 2.429 (4) (Cl^-)	14
$[Pt_2(NH_3)_4(C_5H_4NO)_2(NO_2)_2](NO_3)_2\cdot{}^{1/2}H_2O$	2.576 (1)	2.172 (10) (NO_2^-), 2.168 (11) (NO_2^-)	14
$Na_2[Pt_2(HPO_4)_4(H_2O)_2]$	2.486 (2)	2.151 (11) (H_2O)[a]	15
$K_2[Pt_2(SO_4)_4(OSMe_2)_2]\cdot 4H_2O$	2.471 (1)	2.126 (6) ($OSMe_2$)[a]	16
$[Et_4N]_2[Pt_2(H_2PO_4)_2(HPO_4)_2Cl_2]\cdot H_2O$	2.529 (1)	2.448 (4) (Cl^-)[a]	15
$[pyH][Pt_2(H_2PO_4)(HPO_4)_3(py)_2]\cdot H_2O$	2.494 (1)	2.179 (13) (py)	17

[a] Both Pt-X (axial) distances are symmetry equivalent. [b] This work.

Table VII. Pt-P Distances and P-O-P Angles in $[Pt_2(P_2O_5H_2)_4X_2]^{4-}$ Complexes

	Pt-P, Å	P-O-P, deg	P....P, Å
$K_4[Pt_2(pop)_4]\cdot 2H_2O$	2.320 (5)	133.3 (9)	2.980 (6)
$K_4[Pt_2(pop)_4Br]\cdot 3H_2O$	2.334 (1)	130.2 (3)	2.935 (2)
$K_4[Pt_2(pop)_4CH_3I]\cdot 2H_2O$	2.339 (2)	132.8 (7)	2.936 (4)
$K_4[Pt_2(pop)_4(SCN)_2]\cdot 2H_2O$	2.357 (5)	126.5 (9)	2.889 (7)
$K_4[Pt_2(pop)_4(NO_2)_2]\cdot 2KNO_2\cdot 2H_2O$	2.372 (2)	122.6 (7)	2.864 (4)
$K_4[Pt_2(pop)_4(Im)_2]\cdot 7H_2O$	2.362 (5)	123.2 (9)	2.862 (7)
$K_4[Pt_2(pop)_4Cl_2]\cdot 2H_2O$	2.350 (1)	125.5 (4)	2.873 (3)

Table VIII. Metal-Metal Bond Lengths and $E(\sigma \rightarrow \sigma^*)$ Values for Diplatinum(III,III) Complexes

complex	Pt-Pt, Å	$E(\sigma \rightarrow \sigma^*)$, nm	ref
$[Pt_2(SO_4)_4(OH_2)_2]^{2-}$	2.461 (1)	225	5
$[Pt_2(P_2O_5H_2)_4(OH_2)_2]^{2-}$		245	2d
$[Pt_2(P_2O_5H_2)_4Cl_2]^{4-}$	2.695 (1)	282	2c
$[Pt_2(P_2O_5H_2)_4(Im)_2]^{4-}$	2.745 (1)	250	a
$[Pt_2(P_2O_5H_2)_4(NO_2)_2]^{4-}$	2.754 (1)	313	a
$[Pt_2(P_2O_5H_2)_4(SCN)_2]^{4-}$	2.760 (1)	337	a
$[Pt_2(P_2O_5H_2)_4CH_3I]^{4-}$	2.782 (1)	346	2a

[a] This work.

series in mononuclear platinum(II) complexes.[13] The higher trans influence of SCN^- over the NO_2^- and Im^- ligands indicates that axial σ-electronic delocalization between the Pt-Pt and Pt-X bonds play a substantial role in the weakening of the metal-metal bond. A similar structural trans influence of the axial ligand on the Pt-Pt distances has also been found in the head-to-tail binuclear *cis*-diammineplatinum(III) complexes of α-pyridone,[14] although in that case the changes in the Pt-Pt distance may also result from steric and electronic differences associated with the opposite orientation of the α-pyridonate ligands. The Pt-Pt distances in $[Pt_2(pop)_4X_2]^{4-}$ are generally longer than those found in other symmetrically bridged Pt_2(III, III) complexes (Table VI) and this has previously been attributed to the constraining effect of the bridging ligand.[2a,b] Although a short Pt-Pt bond in $[Pt_2(pop)_4X_2]^{4-}$ increases the Pt($5d_{z^2}$) orbital overlap, it also imposes constraints on the bridging pop ligand. Thus the changes of the Pt-P distance and P-O-P angles with variations in the Pt-Pt distance will reflect the energy barrier caused by the structural changes of the $Pt_2(pop)_4$ barrels in the oxidation of $[Pt_2(pop)_4]^{4-}$ to $[Pt_2(pop)_4X_2]^{4-}$. As the Pt-Pt distance shrinks by 0.143 Å from $[Pt_2(pop)_4]^{4-}$ to $[Pt_2(pop)_4CH_3I]^{4-}$, the average Pt-P distance and P-O-P angle remain relatively constant. However, a further 0.022-Å decrease in the Pt-Pt distance (from $[Pt_2(pop)_4CH_3I]^{4-}$ to $[Pt_2(pop)_4(SCN)_2]^{4-}$) leads to slight structural changes in the $Pt_2(pop)_4$ unit: the P-O-P angles close by about 6° and the Pt-P bonds lengthen by ~0.02 Å (table VII). Notably, both the P-O-P angles and Pt-P distances remain approximately the same from $[Pt_2(pop)_4(SCN)_2]^{4-}$ to $[Pt_2(pop)_4Cl_2]^{4-}$ despite the 0.065-Å difference in the Pt-Pt distance. This indicates that aside from the variation of the metal-metal distance, structural changes of the $Pt_2(pop)_4$ barrel occur when the Pt-Pt bond falls within the range 2.78-2.77 Å. In this case, the P···P distance (i.e., the bite distance of the pop ligand) lies within 2.93-2.89 Å.

Although the hydrogen atoms in the diphosphite ligands were not located, the P—O bond distances in Table V clearly fall into three classes: P—OH, P=O, and P—O (bridging). The P-O (terminal) groups in **1** are orientated in the same sense to form four O-H···O hydrogen bonds around the periphery of each PtP_4 unit (see Figure 3 of ref 2b). In **2** and **3**, however, the P-O (terminal) groups are arranged such that only two O-H···O hydrogen bonds are formed around the corresponding PtP_4 unit, allowing for strong interaction of the binuclear anion with polar groups in its neighborhood. The higher hydration number of **3** as compared to **1** can be rationalized in terms of packing requirements dependent on the relative size of the axial ligands.

As in many other metal-metal-bonded transition-metal complexes, the Pt-X bonds in complexes **1** to **3** are longer than corresponding bonds found in mononuclear platinum(II) complexes. The Pt-S bond in **1** is even longer than that found in β-$[Pt_2Cl_2(PPr_3^n)_2(SCN)_2]$, where the Pt-S bond (2.408 (4) Å) is trans to PPr_3^n.[18] The Pt-N distances in **2** and **3** are ~0.03 Å shorter than that found in *cis*-$[Pt_2(NH_3)_4(C_5H_4NO)_2(NO_2)_2](NO_3)_2$, in agreement with the fact that the latter system has a stronger Pt-Pt bond.[14] The bond lengths and angles of the coordinated SCN^- and NO_2^- groups are normal. The Pt-Pt vector in **2** nearly bisects the O-N-O angle, whereas in **1** the coordinated SCN^- group is slightly tilted away from the Pt-Pt bond [Pt'-Pt-S angle is 172.8 (1)°]. Complex **3** constitutes the first example of a binuclear d^7-d^7 complex with imidazolyl as the axial ligand, which is planar and assumes the usual bond lengths and angles.[19] The C(3)-N(1) distance is longer than C(1)-N(1) and C(1)-N(2) by ~0.1 Å, indicating that the π electrons are not completely delocalized in the ring.

Pt-Pt Bond Distances and $E(\sigma \rightarrow \sigma^*)$ Values. The $E(\sigma \rightarrow \sigma^*)$ of the "long" Pt_2-bonded $[Pt_2(pop)_4(OH_2)_2]^{2-}$ is lower than that of the "short" Pt_2-bonded $[Pt_2(SO_4)_4(OH_2)_2]^{2-}$, in agreement with the qualitative picture that the Pt($5d_{z^2}$) orbitals overlap better with decreasing Pt-Pt separation (Table VIII). A similar observation has been made in the case of analogous dirhodium(II,II) species, where it has been suggested that the difference in $E(\sigma \rightarrow \sigma^*)$ between the short Rh_2-bonded $[Rh_2(OAc)_4]$ and the long Rh_2-bonded $[Rh_2(1,3\text{-diisocyanopropane})_4X_2]^{2+}$ is another manifestation of the different orbital components that contribute to the two types of metal-metal interactions.[4a] We suggest that this argument may also be valid in the case of the diplatinum(III,III) complexes: While the σ and σ^* orbitals of $[Pt_2(SO_4)_4(H_2O)_2]^{2-}$

(13) Appleton, T. G.; Clark, H. C.; Manzer, L. E. *Coord. Chem. Rev.* **1973**, *10*, 335-422.
(14) See for example: Hollis, L. S.; Roberts, M. M.; Lippard, S. J. *Inorg. Chem.* **1983**, *22*, 3637-3644 and references therein.
(15) Bancroft, D. P.; Cotton, F. A.; Falvello, L. R.; Han, S.; Schwotzer, W. *Inorg. Chim. Acta* **1984**, *87*, 147-153.
(16) Cotton, F. A.; Falvello, L. R.; Han, S. *Inorg. Chem.* **1982**, *21*, 2889-2891.
(17) Condor, H. L.; Cotton, F. A.; Falvello, L. R.; Han, S.; Walton, R. A. *Inorg. Chem.* **1983**, *22*, 1887-1891.
(18) Gregory, V. A.; Jarvis, J. A. J.; Kilbroun, B. T.; Owston, P. G. *J. Chem. Soc. A* **1970**, 2770-2774.
(19) Cotton, F. A.; Felthouse, T. R. *Inorg. Chem.* **1981**, *20*, 584-600.

are expected to be primarily Pt($5d_{z^2}$), these levels in $[Pt_2(pop)_4X_2]^{4-}$ may contain substantial contributions from $\pi(P_2O_5H_2)$ and possibly (p_z, s) metal orbitals.[20]

Axial σ-electronic delocalization will be enhanced in $[Pt_2(pop)_4X_2]^{4-}$ complexes in which the energies of $d\sigma$ and $\sigma(X)$ orbitals are not very different. In this circumstance, the $\sigma \rightarrow \sigma^*$ transition is no longer Pt_2 localized, and therefore its energy should not necessarily be related in any simple way to Pt-Pt bond strength.[4b] While decreasing values of $E(\sigma \rightarrow \sigma^*)$ in diplatinum(III,III) diphosphite bridged complexes generally correlate with increasing Pt-Pt bond distances (Table VIII), axial LMCT mixing selectively affects $E(\sigma \rightarrow \sigma^*)$ in certain cases. For example, the Pt-Pt bond distances in $[Pt_2(pop)_4(NO_2)_2]^{4-}$ and $[Pt_2(pop)_4(SCN)_2]^{4-}$ differ by only ~0.006 Å, but $E(\sigma \rightarrow \sigma^*)$ of the latter ion is red shifted by ~2400 cm^{-1} from that of the nitro complex. Also, the very high $E(\sigma \rightarrow \sigma^*)$ of $[Pt_2(pop)_4(Im)_2]^{4-}$ relative to the transition energies of complexes with similar Pt-Pt distances undoubtedly reflects the Pt_2-localized nature of $\sigma \rightarrow \sigma^*$ with Im^- as the axial ligand.

(20) Rice, S. F.; Gray, H. B. *J. Am. Chem. Soc.* **1983**, *105*, 4571-4575.

Acknowledgment. We thank Vince Miskowski for helpful discussions. This research was supported by the Committee of Conference and Research Grants of the University of Hong Kong (C.-M.C. and W.M.L.) and National Science Foundation Grant CHE82-18502 (H.B.G.). Wai-Man Lee acknowledges a graduate studentship from the Croucher Foundation.

Registry No. 1, 102614-74-4; 2, 102630-07-9; 3, 102614-75-5; $K_2[Pt_2(pop)_4(py)_2]$, 102614-76-6; $K_2[Pt_2(pop)_4(nicot)_2]$, 102614-77-7; $[Bu_4N]_4[Pt_2(pop)_4]$, 102630-09-1; $K_4[Pt_2(pop)_4]$, 79716-40-8; Pt, 7440-06-4.

Supplementary Material Available: Imidazolyl H coordinates, anisotropic temperature factors, and structure factor tables for **1-3** (62 pages). Ordering information is given on any current masthead page.

Excited-State Spectra and Lifetimes of Quadruply Bonded Binuclear Complexes: Direct Observation of a New Transient Species following Decay of the $^1(\delta\delta^*)$ State in $Mo_2Cl_4(PBu_3)_4$

Jay R. Winkler,*† Daniel G. Nocera,‡ and Thomas L. Netzel*†,§

Contribution from the Department of Chemistry, Brookhaven National Laboratory, Upton, New York 11973, and Department of Chemistry, Michigan State University, East Lansing, Michigan 48824. *Received August 15, 1985*

Abstract: This paper reports transient absorption kinetics studies in the 10^{-11}-10^{-3} s time range for $[Re_2Cl_8]^{2-}$ (I), $[Mo_2Cl_8]^{4-}$ (II), $Mo_2Cl_4(CH_3CN)_4$ (III), and $Mo_2Cl_4(PBu_3)_4$ (IV) in solution at room temperature. A detailed description of the optical layout and equipment used to measure the kinetics in the 10^{-8}-1 s time range following picosecond excitation is also given. Complexes I-III have small steric barriers to rotation about the M-M bond and upon photoexcitation appear to form $^1(\delta\delta^*)_{staggered}$ metal-metal charge-transfer (MMCT) states in <20 ps. The absorption spectra of $^1(\delta\delta^*)$ MMCT states are shown to have characteristic, strong charge-transfer (CT) bands in the near UV. Complex IV has bulky alkylphosphine groups and should retain its eclipsed geometry in its $^1(\delta\delta^*)$ excited state in noncoordinating solvents. In CH_3CN, IV undergoes some nuclear relaxation in the $^1(\delta\delta^*)$ state with a rate constant of 10^9 s^{-1}. A particularly important result is that in complex IV a nonluminescent transient species is observed at long times (τ ~100 ns) following the decay of the $^1(\delta\delta^*)$ MMCT state.

The study of metal-metal bonding in binuclear complexes continues to be an active area of research in inorganic chemistry.[1-4] An important subset of binuclear complexes pairs two d^4 transition metals in molecules described by ground states with metal-metal quadruple bonds. Numerous experimental[3] and theoretical[4] studies have clarified important aspects of the electronic structures of these molecules, but many fundamental questions remain unanswered.

A simple molecular orbital scheme for d^4-d^4 $[M_2X_8]^{n-}$ complexes with D_{4h} symmetry is illustrated in Figure 1. The eight d-electrons from the two metals fill the four metal-metal bonding orbitals to produce a $(\sigma^2\pi^4\delta^2)$ ground-state configuration and a quadruple bond. This model correctly predicts a diamagnetic ground state for these molecules and an eclipsed (D_{4h}) ligand conformation. It further predicts that a spin and dipole allowed $\delta^2 \rightarrow {}^1(\delta\delta^*)$ excitation should be apparent in the absorption spectra of these molecules. Indeed, bands between 500 and 700 nm in the visible spectra of these molecules have been assigned to this $^1A_{1g} \rightarrow {}^1A_{2u}$ transition.[3] The absorption bands are polarized parallel to the M-M bond (molecular z-axis) and at low temperature resolve into vibrational progressions in the M-M

Table I. State Orderings in d^4-d^4 Complexes: $[Re_2Cl_8]^{2-}$

E^a, eV	states
2.6	$^3A_{2u}(\pi\pi^*)$
2.6	$^1E_g(\pi\delta^*)$
2.2	$^1A_{1g}(\delta^*\delta^*)$:$^1[(xy_A)(xy_A) + (xy_Bxy_B)]$
1.8	$^1A_{2u}(\delta\delta^*)$:$^1[(xy_A)(xy_A)-(xy_Bxy_B)]$
1.8	$^3E_g(\pi\delta^*)$
0.4	$^3A_{2u}(\delta\delta^*)$:$^3[(xy_A)(xy_B)]$
0	$^1A_{1g}$:$^1[(xy_A)(xy_B)]$

[a] Reference 4c.

(1) Cotton, F. A.; Walton, R. A. *Multiple Bonds Between Metal Atoms*; Wiley: New York, 1982.
(2) (a) Chisholm, M. H.; Cotton, F. A. *Acc. Chem. Res.* **1978**, *11*, 356. (b) Cotton, F. A. In *Transition Metal Chemistry, Procedure Workshop*; Müller, A.; Diemann, E., Eds.; Verlag Chem: Weinheim, Germany, 1981; p 51. (c) *Reactivity of Metal-Metal Bonds*; Chisholm, M. H., Ed. ACS Symposium Series; American Chemical Society: Washington, DC 1981; Vol. 155. (d) Chisholm, M. H.; Rothwell, I. P. *Prog. Inorg. Chem.* **1982**, *29*, 1. (e) Chisholm, M. H. *Polyhedron* **1983**, *2*, 681. (f) Meyer, T. J.; Caspar, J. V. *Chem. Rev.* **1985**, *85*, 187.

† Brookhaven National Laboratory.
‡ Michigan State University.
§ Present Address: Amoco Corporation, Corporate Research Department, Amoco Research Center, Post Office Box 400, Naperville, IL 60566.

0002-7863/86/1508-4451$01.50/0